Title

A Quantitative Assessment of Wound Healing With Oxygenated Micro/Nanobubbles in a Preclinical Burn Model

Journal

Annals of Plastic Surgery, 87(4)

ISSN

0148-7043

Authors

Sayadi, Lohrasb R
Rowland, Rebecca
Naides, Alexandra
et al.

Publication Date

2021-10-01

DOI

10.1097/sap.0000000000003017

Peer reviewed

HHS Public Access

Author manuscript

Ann Plast Surg. Author manuscript; available in PMC 2022 October 01.

Published in final edited form as:

Ann Plast Surg. 2021 October 01; 87(4): 421–426. doi:10.1097/SAP.0000000000003017.

A Quantitative Assessment of Wound Healing with Oxygenated Micro/nanobubbles in a Preclinical Burn Model

Lohrasb R. Sayadi[1], **Rebecca Rowland**[2], **Alexandra Naides**[1], **Luke Tomlinson**[1], **Adrien Ponticorvo**[2], **Anthony J. Durkin**[2,3], **Alan D. Widgerow**[1]

[1]Center for Tissue Engineering, Department of Plastic Surgery, University of California, Irvine, 200 S. Manchester Ave., Suite 650, Orange, CA 92868

[2]Beckman Laser Institute and Medical Clinic, University of California, Irvine, 1002 Health Sciences Road East, Irvine, CA 92617

[3]Department of Biomedical Engineering, University of California, Irvine, 3120 Natural Sciences II, Irvine, CA 92697

Abstract

Background: Burns are devastating injuries, carry significant morbidity, and require long-term treatment or multiple reconstructive procedures. Wound healing and secondary insults caused by burn wound conversion is amendable to therapeutic intervention, where ischemia has been cited as one of the major factors[1]. Halting injury progression in the zone of stasis is crucial as conversion creates increased burn surface area, depth, leading to local and systemic consequences[2]. Oxygen carrying Micro/nanobubbles, (MNB(O_2)), offer a novel technology which can be used to effectively deliver oxygen to burn wounds and potentially counteract burn wound ischemia.

Methods: Topical irrigation with MNB(O_2) of full-thickness burns wounds on a rat model (*n=3*) were compared against saline treated controls (*n=3*). Tissue structure (reduced scattering coefficient, μ_s'), oxyhemoglobin concentration (cHbO_2), and tissue perfusion were quantified over the course of 28 days through spatial frequency domain imaging (SFDI) and laser speckle imaging (LSI). Histological samples taken at the end of the experiment were examined for evidence of wound healing.

Results: Findings in this preliminary study showed hastened healing with significant differences in SFDI-measured μ_s' during wound healing (days 11-28) in MNB(O_2) group. The healing 'tipping point' appeared to occur at days 9-11 with increased collagen organization, increased cHbO_2 occurring around that period confirming the gross healing improvements observed. In addition, histological evidence indicated that only the MNB(O_2) burns had reached the remodeling phase by the end of 28-day study period.

Corresponding Author: **Dr. Alan D. Widgerow – MBBCh(MD); MMed(MHS); FCS (Plast); FACS**, Professor Plastic Surgery, Director Center for Tissue Engineering, Dept. of Plastic Surgery, University of California, Irvine (Suite 108a Building 55, 101 S. City Dr, Orange CA, 92868- Tel 714.456.3482 Fax: 714-456-7718, awidgero@uci.edu).

Conflict of interest: Dr. Durkin has a financial interest in modulim, Inc., which developed the OxImager RS®. However, Dr. Durkin does not participate in the management of modulim,and has not shared these results with the company. Conflicts of interest have been disclosed and managed in accordance with University of California and NIH policies. The other authors have no financial interests or commercial associations that might pose or create a conflict of interest with the information presented in this article.

Conclusions: These preliminary findings propose the potential of MNB(O_2) as a topical method for improving burn wound healing.

1. INTRODUCTION

It is estimated that over 330,000 burn patients require medical treatment per year in the United States[3]. Of these, 40,000 patients will require hospitalization[4], often in one of the 128 US burn centers. As such, expedient and effective treatment is critical to burn wound care, in order to decrease patient's length of stay, and improve their cosmetic and functional outcomes[5,6]. Tissue ischemia and perturbations in tissue oxygen delivery are cited as factors involved in burn wound conversion, where burn severity increases during the first 48 hours post-injury[2]. Ameliorating local ischemia in burn injuries increases the area of salvageable tissue, and thus, maintaining an appropriate level of oxygen in burns is a therapeutic goal[1,7]. To this end, hyperbaric oxygen therapy (HBOT) and topical oxygen therapy (TOT) have been developed in an attempt to improve oxygenation of tissue and accelerate the process of wound healing[8,9]. However, these technologies can be expensive, lack portability and may have potentially serious side-effects[10-14].

Due to the barriers associated with the aforementioned technologies, alternative approaches are sought to deliver oxygen to wounds. Micro/nanobubbles (MNBs) are miniature gaseous bubbles in fluid that offer an innovative new approach for improving burn oxygenation[8]. Microbubbles have diameters between 1-100μm, whereas nanobubbles are less than 1μm in diameter[15]. These bubbles can be generated within minutes by exposing a mixture of fluid and gas to shear forces. The properties which make MNBs unique and contribute to their versatility are their high stability in water, slow rise, gradual shrinkage and high affinity for oxygen[8,15]. Since their internal pressure is much higher than that of their local environment, MNBs promote the solubility of oxygen into the liquid in which they are produced which can reach oxygen pressures up to 800 mmHg.

Previous studies by our group have characterized oxygen carrying capacity of MNBs overtime as well as their stability in solution and efficacy as an oxygen delivery vehicle to transplantable tissues[16]. Other groups have demonstrated that MNBs can counteract the hypoxia dependent dysregulation of the MMP/TIMP balance in human keratinocytes and reduce HIF-1 alpha signaling, both of which have important implications in wound healing[17]. While interest in MNBs is growing, their implementation in medicine and their application in wound healing still remains to be fully explored.

The aim of this preclinical pilot study was to determine the efficacy of MNBs in the treatment of burn wounds. To effectively ascertain changes related to burn wound physiology with MNB application, an objective means of measuring wound healing overtime was utilized. Spatial frequency domain imaging (SFDI) is a validated non-contact based optical modality which captures wound information such as structure, collagen content and vascularity [18,19,20,21,22]. This technology was paired with laser speckle imaging (LSI), a noninvasive imaging technique which quantifies wound perfusion in burns and there periphery[23,24]. Here in SFDI, LSI and histologic analysis was used to assess full-thickness

rodent burn wounds treated with either topical MNB or saline irrigation over the course of 28 days.

2. MATERIALS AND METHODS

2.1 Micro/nanobubbles Generation

Oxygen carrying MNBs, MNB(O_2), were produced in saline using a shear generation system based upon a gear pump design described previously[25]. This design first pre-mixes saline and compressed oxygen in a metered fashion, followed by shear generation and subsequent controlled decompression to produce MNB(O_2).

After MNB(O_2) generation, a 1ml aliquot of the MNB(O_2) solution was analyzed at 25°C. The particle count and size analysis were measured using the *NanoSight* Nanoparticle Tracking System (NanoSight NS300, Malvern instruments, Worcestershire, United Kingdom). The MNB(O_2) solutions were thermostatically-maintained for 30min, post-generation, to quantify the sub 2μm bubbles in the solutions. The average measured size of the MNBs generated was 167.3 ± 13.0nm, with a concentration of $1.46 \times 10^8 \pm 2.49 \times 10^7$ MNB(O_2) per milliliter.

Following the generation of the MNB(O_2) solution, the dissolved oxygen content (pO_2) of the solution was measured as previously described [15,26]. The dissolved oxygen level (mmHg) of the MNB(O_2) solution, shown in Figure 1, was evaluated over a 10-hour period to demonstrate the oxygen tension of the solution during the wound treatment window.

2.2 Burn Wound Generation and Treatment Protocol

Six male (*n=6*) Sprague Dawley rats (Charles River Laboratories Inc., San Diego, CA), weighing between 320-380g, were selected as the animal model. Three of the (*n=3*) animals were choose at random to receive topical irrigation of MNB(O_2) and the remaining three animals (*n=3*) served as controls and received topical irrigation of saline. All animal work was completed under a study protocol approved by the UC Irvine Institutional Animal Care and Use Committee (IACUC AUP-17-137). Twenty-four hours prior to study initiation, hair was cleared from the dorsum of all animals. To generate burns 3 cm diameter cylindrical brass burn tool was heated to 100°C in a dry bath incubator (Thermo Fisher Scientific, MA). Following a validated protocol for contact burns, full-thickness burn wounds were created by holding the burn tool against the rats' dorsum for 12 seconds maintaining a constant pressure while animals were under anesthesia[20,21,27,28].

Each animal was treated with the respective solutions over 12 days, beginning immediately after burn injury on day 0. The animals were treated continuously over the first 72 hours post-burn, then in alternating 24-hour periods for the remainder of the 12-day treatment period. Alternating 24-hour wet dry cycles were implemented to allow for animal self-grooming. To achieve topical irrigation, the animals were affixed to a custom infusion harness, modified from the OMNI single harness and tether system (SAI Infusion Technologies, Lake Villa, IL), as shown in Figure 2. A catheter was positioned over the burn wound on the dorsum, and the tether was connected to a syringe pump (New Era Pump

Systems, Inc., Farmingdale, NY). The pump was set to deliver 60 milliliters of topical fluid ($MNB(O_2)$ or saline solution) on the wound site over 12 hours.

2.3 Spatial Frequency Domain Imaging (SFDI)

Spatial frequency domain imaging (SFDI) was used to assess burn wound healing in $MNB(O_2)$ and saline treated burns by quantitatively assessing collagen organization through measurements of the reduce scattering coefficient (μ_s'), and tissue oxygenation through measurements of absorption (μ_a). These measurements were collected before the burn and on days 0, 2, 4, 7, 9, 11, 14, 18, 21, and 28. SFDI, a noncontact and wide-field imaging method, measures optical properties by projecting sinusoidal patterns at multiple wavelengths and spatial frequencies[29,30]. The reflectance measurements were calibrated using a silicone tissue-simulating phantom having known optical properties and converted into values of reduced scattering coefficient (μ_s') and absorption coefficient (μ_a). The reduced scattering coefficient can be used to quantitatively measure changes due to collagen denaturation or remodeling, whereas the absorption coefficient can be used to deduce chromophore concentrations related to oxyhemoglobin (HbO_2) and deoxyhemoglobin (Hbr). In the present study our team employed the OxImager RS® SFDI device (modulim, Inc., Irvine, CA) which measures tissue reflectance over a wide field of view (20x15cm) at 8 wavelengths (471, 526, 591, 621, 659, 691, 731, and 851nm) and 5 spatial frequencies (0, 0.05, 0.10, 0.15, and 0.20mm^{-1})[29]. Data processing was performed using the MI Analysis v1.14.21 software suite (modulim Inc., Irvine, CA) and Matlab (R2018a, MathWorks, Inc., Natick, MA), for analysis of individual regions of interest (ROIs) within each burn.

2.4 Laser Speckle Imaging (LSI)

Laser speckle imaging (LSI) measurements were taken to determine differences in tissue perfusion in $MNB(O_2)$ and saline treated burns and was performed every other day throughout the full course of the study. An 809nm laser (Ondax, Monrovia, CA) was used to illuminate each burn region. For every measurement, 50 raw speckle images were collected with a Nuance™ camera system (CRI Inc., Woburn, MA) over a 0.089x0.065 m2 field of view at a T = 10ms exposure. Raw speckle data was converted to Speckle Flow Index (SFI), using a method described previously[24].

2.5 Histology

On day 28 all animals were sacrificed via CO_2 inhalation followed by cervical dislocation, and 6 mm punch biopsies were taken from each burn wound paying particular attending on capturing the most representative area for histological analysis. The tissue was fixed routinely, stained with hematoxylin and eosin and assessed for evidence of re-epithelialization, hair follicle growth, eschar, granulation, and epidermal thickness by a blinded technician[31]. In areas of re-epithelialization, the distances between the epidermal-dermal junction and stratum corneum junction were measured at multiple evenly spaced points (5/cross-section) in a high-power view to determine epidermal thickness. Increased epidermal thickness has been used as a metric related to scar formation and the early remodeling phase of wound healing, while thinner epidermis has been indicative of the later remodeling phase or lack of hypertrophic scarring[32-34].

2.6 Statistical Analysis

A 1 cm^2 region was chosen from the center of each burn and monitored through the course of the experiment, for mean values of reduced scattering and chromophore concentration. Mean optical property and epidermal thickness values measured from the MNB(O_2) treated burns were compared to the those obtained for the control population at each imaging time point using a two-sample t-test. A p-value less than 0.05 was considered statistically significant for this study. A power analysis for a two-sample t-test performed on the mean reduced scattering values measured at the end of treatment. These day 11 measurements (control mean: 1.032 mm^{-1}, control standard deviation: 0.1715 mm^{-1}, test mean: 1.668 mm^{-1}, test standard deviation: 0.1596 mm^{-1}) indicated that $n=3$ was sufficient sample size for each group given a 0.9 power of the test.

3. RESULTS

3.1 Gross Observations of Wound Area

On gross examination of the burn wounds throughout the study, we observed quicker eschar formation in the MNB(O_2) treatment group which separated with hastened healing in this group from day 11 onwards (Figure 3). Eschars which developed in the saline treated burns were thinner than those developed in MNB treatment group, although measurements of eschar thickness were not performed over concern for disrupting the wounds.

3.1 Collagen Organization

SFDI imaging was utilized to better assess structural properties of the burn wounds over the course of the study. A statistically significant ($p<0.05$) improvement in collagen organization (reduced scattering coefficient) was observed in MNB(O_2) treated burns when compared to saline treated burns starting day 11 and up until study termination on day 28 (Figure 4, Table 1 Supplemental Digital Content 1).

3.2 Oxyhemoglobin Concentration and Tissue Perfusion

Oxyhemoglobin concentration ($cHbO_2$) was measured in both MNB(O_2) and saline treated burns throughout the course of the study. Unfortunately, eschar formation created difficulties reliably measuring $cHbO_2$ using SDFI and LSI in the underlying dermis prior to eschar separation (days 3 – 11). At day 2, there was higher $cHbO_2$ in some of the MNB(O_2) treated cases, but a two-sample t-test indicated no significant difference ($p = 0.516$). However, on day 14, after removal of the eschar, MNB(O_2) treated burns showed a statistically significant increase in $cHBO_2$ when compared to the saline group ($p = 0.024$) (Figure 5, Supplemental Digital Content 2). At day 28, $cHBO_2$ was higher in the saline-treated burns than the MNB(O_2) treated burns ($p = 0.041$). LSI-measured perfusion levels between MNB(O_2) treated burns were also compared to saline burns at the 2, 14, 21- and 28-day post-burn time points. There was no statistically significant difference in perfusion levels during these time points between the two groups (Supplemental Digital Content 3).

3.4 Histological Analysis

Histological examination of tissue obtained at day 28 demonstrated evidence of improved wound healing in MNB(O_2) treated burns over the saline-treated control (Figure 6). Mean epidermal thickness for the MNB(O_2)-treated animals was 0.053mm (+/− 0.017), and the 0.16mm (+/− 0.079), which was found to be statistically significant (p<0.001). Two of the MNB(O_2) sections showed complete re-epithelialization and keratinization over the length of the section, while the saline-treated animals only showed 50-75 precent re-epithelialization over the entirety of a section. The MNB(O_2) burns had more evidence of wound remodeling, where one sample had as little as 50 precent granulation tissue in the dermis. The saline-treated burns showed at least 75 precent granulation tissue throughout the extent of the dermis. Among the imaged sections for the six animals, four instances of areas of hair follicle/adnexal structure regeneration were identified in the MNB(O_2) treated cohort, while only one instance was identified in the saline-treated animals.

4. DISCUSSION

Since the advent of hyperbaric oxygen therapy (HBOT) by Henshaw in 1662, medicine has sought to improve oxygen delivery to poorly healing tissue[35]. It was once believed that the sole source of oxygen available for biochemical processes in wound healing derived from the systemic circulation. It is now thought, and supported by several studies, that skin can utilize oxygen from the atmosphere[36-38]. In vitro studies show that oxygen passes through the intact stratum corneum down to a depth of approximately 0.30 mm in the superficial dermis[37,38]. Similarly, studies have shown that the necessary transcutaneous oxygen level ($TcpO_2$) for normal skin is 30 mmHg or greater with levels less than 30 mmHg often leading to poor wound healing outcomes[39].

Micro/nanobubbles (MNBs) are miniature gaseous bodies in fluid which can deliver oxygen to wounds. The properties which make MNBs unique and contribute to their versatility are their stability in water, slow rise, gradual shrinkage, and collapse[40]. Because their internal pressure is much higher than that of their local environment, MNBs promote the solubility of their internal gas into the liquid in which they are produced[17,40-43] (Figure 1). Additionally, their negatively charged surface not only prevents them from merging together, thus losing their efficacy, but also attracts particulate matter and thereby assists in the removal of debris[40,44]. Finally, florescent-labeling has shown that nanobubbles are internalized by cells, including keratinocytes in the skin [41-43,45-47]. The aim of the present study was to determine whether micro/nanobubbles could improve burn healing in the rodent model.

We observed that the eschars of MNB(O_2) treated burns separated after study day 11, leaving behind re-epithelialized skin (Figure 3). The eschars limited our ability to measure $cHbO_2$ at early time points, however the scattering coefficient data demonstrated a healing tipping point between 9 and 11 days where the MNB(O_2) group displayed increased collagen formation/organization (Figure 4, Table 1, Supplemental Digital Content 1) which persisted until study termination and a significantly improved $cHbO_2$ after eschar separation at day 14 when compared to saline treated counterparts ($p<0.05$, Figure 5, Supplemental Digital Content 2). In addition, we did not observe a significant difference in physiologic

perfusion levels between the two groups which supports the hypothesis that differences in tissue oxygenations were related to MNB(O_2) treatment rather than increase vascular oxygen delivery to the tissue (Supplemental Digital Content 3). Histological analysis of the burn wounds at day 28 demonstrated that MNB(O_2) treated burns had thinner and more organized epidermis ($p<0.05$), evidence of improved reepithelization, less granulation tissue and greater number of hair follicles when compared to saline treated counterparts further supporting the improved healing quantified by SFDI and LSI (Figure 6).

Taken together the results indicate that Micro/nanobubbles significantly improve the physical properties of the burn wounds with improved collagen organization, hair regeneration and reepithelization being the hallmarks. In addition, burn wound oxygenation improved in the experimental group, MNB (O_2) in the same time period. Given our findings we believe that MNBs can be used to improve oxygenation and thereby healing of a wide variety of ischemic tissue including burns and chronic wounds. The portability of MNB generation devices and preservation of MNB oxygen carrying capacity in closed systems make them suitable for clinical use as an adjunctive therapy. Clinically MNBs can be applied through wet-to-dry dressings, paired with Negative Pressure Wound therapy with Instillation (NPWT-i) and used in hydrotherapy.

We recognize the limitations of this pre-clinical study which include a small sample size, inability to definitively ascertain the oxygenation of the tissue in areas of eschar formation, lack of histological data at additional time points. However, our team was able to achieve statistical significance on key parameters related to healing as demonstrated by improved collagen organization of the burn wounds and oxygenation at specific time points. The limitations of optical technology in penetrating wound eschar in order to garner information about the underlying burn is clearly an area that requires further investigation and improvement. However, other modalities for measuring tissue oxygenation such as Clark based probes can be invasive and only provide data on the oxygenation of the wound periphery not the wound itself. It is unlikely that increasing sample size would ameliorate these technological limitations. Future studies planned by our group aim on increasing sample size such that we can histologically assess the wound at different time points and correlated these findings with data obtained by our non-contact based imagining systems. In addition, treatment arms such as HBOT and TOT groups can be added to draw comparisons. Nevertheless, this study is the first to investigate the used of Micro/nanobubbles as a solution for oxygen delivery to burn wounds and offers promising data which can be expanded upon by the scientific community.

Supplementary Material

Refer to Web version on PubMed Central for supplementary material.

Acknowledgments

We thankfully recognize support from the NIH, including NIBIB P41EB015890 (A Biomedical Technology Resource). We also recognize support from NIGMS grant R01GM108634-01A which enabled the use of the OxImager RS®. The content is solely the responsibility of the authors and does not necessarily represent the official views of the NIGMS, NIBIB or NIH. In addition, this material is based, in-part, upon rat burn imaging work supported by the Air Force Office of Scientific Research under award number FA9550-14-1-0034. Any opinions,

findings, and conclusions or recommendations expressed in this material are those of the authors and do not necessarily reflect the views of the United States Air Force. We also thank the Arnold Beckman Foundation.

List of Abbreviations

MNB	Micro/nanobubbles
MNB(O_2)	Oxygen filled Micro/nanobubbles
HBOT	Hyperbaric Oxygen Therapy
TOT	Topical Oxygen Therapy
MMP	Matrix metalloproteinases
TIMP	Tissue inhibitors of metalloproteinases
HIF −1 Alpha	Hypoxia Inducible Factor 1 Subunit Alpha
NPWT-i	Negative Pressure Wound Therapy with instillation
SFDI	Spatial frequency domain imaging
LSI	Laser speckle imaging

References:

1. Rodriguez PG, Felix FN, Woodley DT, Shim EK. The role of oxygen in wound healing: a review of the literature. Dermatologic surgery : official publication for American Society for Dermatologic Surgery [et al]. 2008;34(9):1159–1169.
2. Devgan L, Bhat S, Aylward S, Spence RJ. Modalities for the assessment of burn wound depth. J Burns Wounds. 2006;5:e2. [PubMed: 16921415]
3. National Hospital Ambulatory Medical Care Survey: 2016 Emergency Department Summary Tables. CDC/National Center for Health Statistics; 2016. https://www.cdc.gov/nchs/data/nhamcs/web_tables/2016_ed_web_tables.pdf.
4. ABA. Burn Incident Fact Sheet http://ameriburn.org/who-we-are/media/burn-incidence-fact-sheet/. Accessed June 19, 2019.
5. Lawrence JW, Mason ST, Schomer K, Klein MB. Epidemiology and impact of scarring after burn injury: a systematic review of the literature. Journal of burn care & research : official publication of the American Burn Association. 2012;33(1):136–146. [PubMed: 22138807]
6. Johnson RM, Richard R. Partial-thickness burns: identification and management. Adv Skin Wound Care. 2003;16(4):178–187; quiz 188-179. [PubMed: 12897674]
7. Salibian AA, Rosario ATD, Severo LAM, et al. Current concepts on burn wound conversion-A review of recent advances in understanding the secondary progressions of burns. Burns : journal of the International Society for Burn Injuries. 2016;42(5):1025–1035. [PubMed: 26787127]
8. Sayadi LR, Banyard DA, Ziegler ME, et al. Topical oxygen therapy & micro/nanobubbles: a new modality for tissue oxygen delivery. International Wound Journal. 2018;15(3):363–374. [PubMed: 29314626]
9. Sen CK, Khanna S, Gordillo G, Bagchi D, Bagchi M, Roy S. Oxygen, oxidants, and antioxidants in wound healing: an emerging paradigm. Annals of the New York Academy of Sciences. 2002;957:239–249. [PubMed: 12074976]
10. Heyboer M 3rd, Sharma D, Santiago W, McCulloch N. Hyperbaric Oxygen Therapy: Side Effects Defined and Quantified. Adv Wound Care (New Rochelle). 2017;6(6):210–224. [PubMed: 28616361]

11. Weaver LK, Churchill S. Pulmonary edema associated with hyperbaric oxygen therapy. Chest. 2001;120(4):1407–1409. [PubMed: 11591590]
12. Heyboer Rd M, Wojcik SM, Smith G, Santiago W. Effect of hyperbaric oxygen therapy on blood pressure in patients undergoing treatment. Undersea Hyperb Med. 2017;44(2):93–99. [PubMed: 28777899]
13. Gordillo GM, Sen CK. Revisiting the essential role of oxygen in wound healing. American journal of surgery. 2003;186(3):259–263. [PubMed: 12946829]
14. Maeda Y, Hosokawa S, Baba Y, Tomiyama A, Ito Y. Generation mechanism of micro-bubbles in a pressurized dissolution method. Exp Therm Fluid Sci. 2015;60:201–207.
15. Matsuki N, Ichiba S, Ishikawa T, et al. Blood oxygenation using microbubble suspensions. Eur Biophys J Biophy. 2012;41(6):571–578.
16. Sayadi LR, Alexander M, Sorensen AM, et al. Micro/nanobubbles: Improving Pancreatic Islet Cell Survival for Transplantation. Annals of plastic surgery. 2019;83(5):583–588. [PubMed: 31232817]
17. Sayadi LR, Banyard DA, Ziegler ME, et al. Topical oxygen therapy & micro/nanobubbles: a new modality for tissue oxygen delivery. Int Wound J. 2018;15(3):363–374. [PubMed: 29314626]
18. Cuccia DJ, Abookasis D, Frostig RD, Tromberg BJ. Quantitative In Vivo Imaging of Tissue Absorption, Scattering, and Hemoglobin Concentration in Rat Cortex Using Spatially Modulated Structured Light. In: nd, Frostig RD, eds. In Vivo Optical Imaging of Brain Function. Boca Raton (FL)2009.
19. Cuccia DJ, Bevilacqua F, Durkin AJ, Ayers FR, Tromberg BJ. Quantitation and mapping of tissue optical properties using modulated imaging. Journal of biomedical optics. 2009;14(2):024012. [PubMed: 19405742]
20. Nguyen JQ, Crouzet C, Mai T, et al. Spatial frequency domain imaging of burn wounds in a preclinical model of graded burn severity. Journal of biomedical optics. 2013;18(6):66010. [PubMed: 23764696]
21. Ponticorvo A, Burmeister DM, Rowland R, et al. Quantitative long-term measurements of burns in a rat model using Spatial Frequency Domain Imaging (SFDI) and Laser Speckle Imaging (LSI). Lasers in surgery and medicine. 2017;49(3):293–304. [PubMed: 28220508]
22. Saidian M, Lakey JRT, Ponticorvo A, et al. Characterisation of impaired wound healing in a preclinical model of induced diabetes using wide-field imaging and conventional immunohistochemistry assays. Int Wound J. 2019;16(1):144–152. [PubMed: 30273979]
23. Crouzet C, Nguyen JQ, Ponticorvo A, Bernal NP, Durkin AJ, Choi B. Acute discrimination between superficial-partial and deep-partial thickness burns in a preclinical model with laser speckle imaging. Burns : journal of the International Society for Burn Injuries. 2015;41(5):1058–1063. [PubMed: 25814299]
24. Ramirez-San-Juan JC, Ramos-Garcia R, Guizar-Iturbide I, Martinez-Niconoff G, Choi B. Impact of velocity distribution assumption on simplified laser speckle imaging equation. Optics express. 2008;16(5):3197–3203. [PubMed: 18542407]
25. Klopfer M. Micro and Nanobubbles for Wound Healing Applications: Biomedical Engineering, University of California, Irvine; 2015.
26. Kakiuchi K, Matsuda K, Harii N, Sou K, Aoki J, Takeoka S. Establishment of a total liquid ventilation system using saline-based oxygen micro/nano-bubble dispersions in rats. Journal of Artificial Organs. 2015;18(3):220–227. [PubMed: 25854604]
27. Gaines C, Poranki D, Du W, Clark RA, Van Dyke M. Development of a porcine deep partial thickness burn model. Burns : journal of the International Society for Burn Injuries. 2013;39(2):311–319. [PubMed: 22981797]
28. Singer AJ, Taira BR, Lin F, et al. Curcumin reduces injury progression in a rat comb burn model. Journal of burn care & research : official publication of the American Burn Association. 2011;32(1):135–142. [PubMed: 21088615]
29. Cuccia DJ, Bevilacqua F, Durkin AJ, Tromberg BJ. Modulated imaging: quantitative analysis and tomography of turbid media in the spatial-frequency domain. Optics letters. 2005;30(11):1354–1356. [PubMed: 15981531]

30. Cuccia DJ. Spatial Frequency Domain Imaging (SFDI): A technology overview and validation of an LED-based clinic-friendly device. Emerging Digital Micromirror Device Based Systems and Applications Iv. 2012;8254.
31. Meyerholz DK, Piester TL, Sokolich JC, Zamba GK, Light TD. Morphological parameters for assessment of burn severity in an acute burn injury rat model. Int J Exp Pathol. 2009;90(1):26–33. [PubMed: 19200248]
32. Katou-Ichikawa C, Nishina H, Tanaka M, et al. Participation of Somatic Stem Cells, Labeled by a Unique Antibody (A3) Recognizing both N-glycan and Peptide, to Hair Follicle Cycle and Cutaneous Wound Healing in Rats. Int J Mol Sci. 2020;21(11).
33. Choi YH, Kim KM, Kim HO, Jang YC, Kwak IS. Clinical and histological correlation in post-burn hypertrophic scar for pain and itching sensation. Ann Dermatol. 2013;25(4):428–433. [PubMed: 24371389]
34. Limandjaja GC, van den Broek LJ, Waaijman T, et al. Increased epidermal thickness and abnormal epidermal differentiation in keloid scars. The British journal of dermatology. 2017;176(1):116–126. [PubMed: 27377288]
35. Kindwall EKindwall EP WH. A History of Hyperbaric Medicine 2nd ed. Flagstaff, Ariz: Best Publishing 2002.
36. Stucker M, Struk A, Altmeyer P, Herde M, Baumgartl H, Lubbers DW. The cutaneous uptake of atmospheric oxygen contributes significantly to the oxygen supply of human dermis and epidermis. J Physiol-London. 2002;538(3):985–994. [PubMed: 11826181]
37. Penneys R, Felder W, Christophers E. The passage of oxygen through isolated sheets of human stratum corneum. Proc Soc Exp Biol Med. 1968;127(4):1020–1022. [PubMed: 5655639]
38. Gruber RP, Heitkamp DH, Billy LJ, Amato JJ. Skin permeability to oxygen and hyperbaric oxygen. Archives of surgery. 1970;101(1):69–70. [PubMed: 5419733]
39. Heng MC, Harker J, Bardakjian VB, Ayvazian H. Enhanced healing and cost-effectiveness of low-pressure oxygen therapy in healing necrotic wounds: a feasibility study of technology transfer. Ostomy Wound Manage. 2000;46(3):52–60, 62. [PubMed: 10788918]
40. Matsuki N, Ichiba S, Ishikawa T, et al. Blood oxygenation using microbubble suspensions. European biophysics journal : EBJ. 2012;41(6):571–578. [PubMed: 22476882]
41. Khadjavi A, Magnetto C, Panariti A, et al. Chitosan-shelled oxygen-loaded nanodroplets abrogate hypoxia dysregulation of human keratinocyte gelatinases and inhibitors: New insights for chronic wound healing. Toxicol Appl Pharmacol. 2015;286(3):198–206. [PubMed: 25937238]
42. Basilico N, Magnetto C, D'Alessandro S, et al. Dextran-shelled oxygen-loaded nanodroplets reestablish a normoxia-like pro-angiogenic phenotype and behavior in hypoxic human dermal microvascular endothelium. Toxicol Appl Pharmacol. 2015;288(3):330–338. [PubMed: 26276311]
43. Cavalli R, Bisazza A, Giustetto P, et al. Preparation and characterization of dextran nanobubbles for oxygen delivery. Int J Pharm. 2009;381(2):160–165. [PubMed: 19616610]
44. Tsuge H Micro- and Nanobubbles: Fundamentals and Applications. Singapore: Pan Stanford Publishing; 2014.
45. Tyssebotn IM, Lundgren CE, Olszowka AJ, Bergoe GW. Hypoxia due to shunts in pig lung treated with O2 and fluorocarbon-derived intravascular microbubbles. Artif Cells Blood Substit Immobil Biotechnol. 2010;38(2):79–89. [PubMed: 20196682]
46. Magnetto C, Prato M, Khadjavi A, et al. Ultrasound-activated decafluoropentane-cored and chitosan-shelled nanodroplets for oxygen delivery to hypoxic cutaneous tissues. Rsc Adv. 2014;4(72):38433–38441.
47. Kakiuchi K, Matsuda K, Harii N, Sou K, Aoki J, Takeoka S. Establishment of a total liquid ventilation system using saline-based oxygen micro/nano-bubble dispersions in rats. J Artif Organs. 2015;18(3):220–227. [PubMed: 25854604]

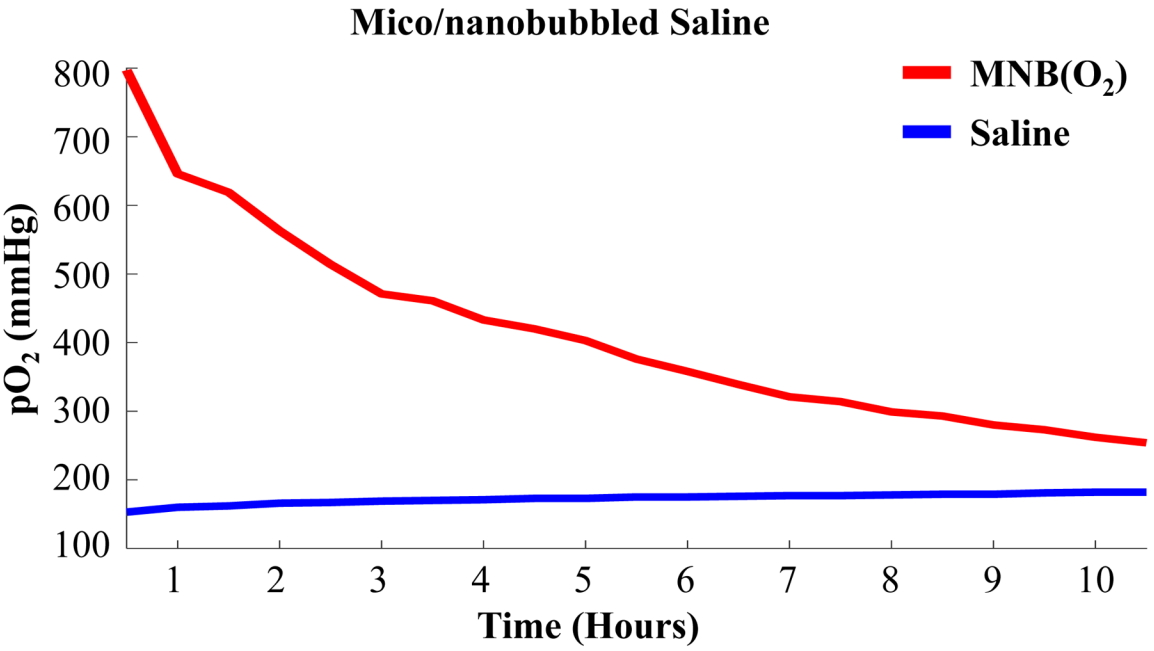

Figure 1:
$MNB(O_2)$ oxygen carrying capacity (red) vs saline (blue) over 10-hour period at room temperature 25°C (*n=4*).

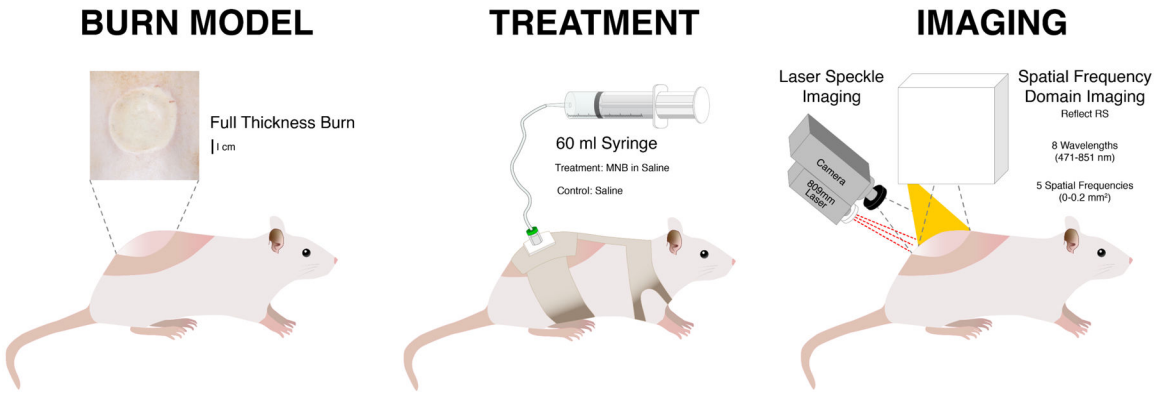

Figure 2:

Full-thickness burn wounds were treated with either MNB(O_2) or saline control. A custom infusion harness was used to confine the treatment to the burn region. Burns were assessed using SFDI and LSI.

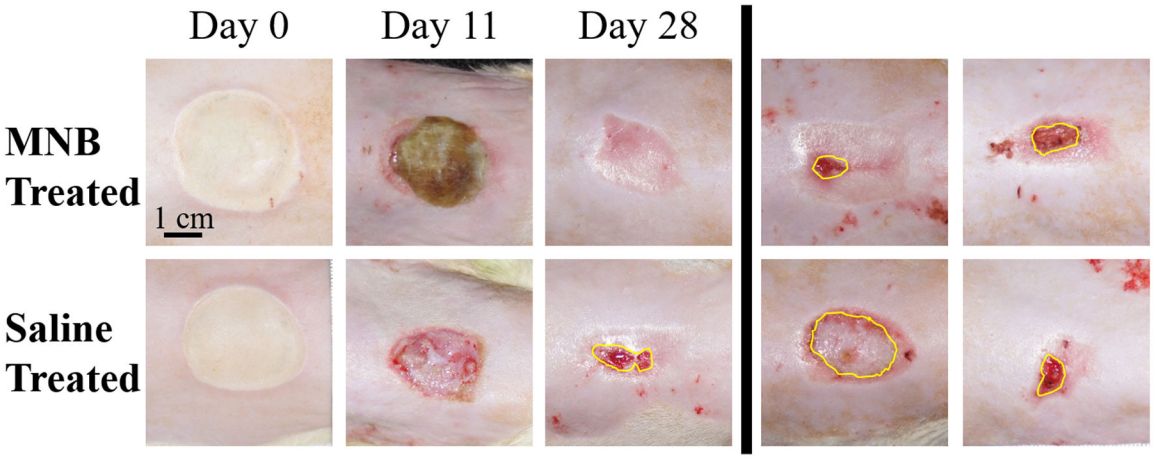

Figure 3:

Gross appearance of burn wounds treated with either topical MNB(O_2) or saline irrigation over the course of 28 days. Last two columns correlate to day 28 wounds in remaining animals in each cohort. On gross examination of the wounds the MNB (O_2) treated burns developed a mature eschar earlier than the saline treated burns. Average size of non-epithelialized areas – 1.51 cm^2 saline vs 0.35 cm^2 MNB(O_2) at day 28.

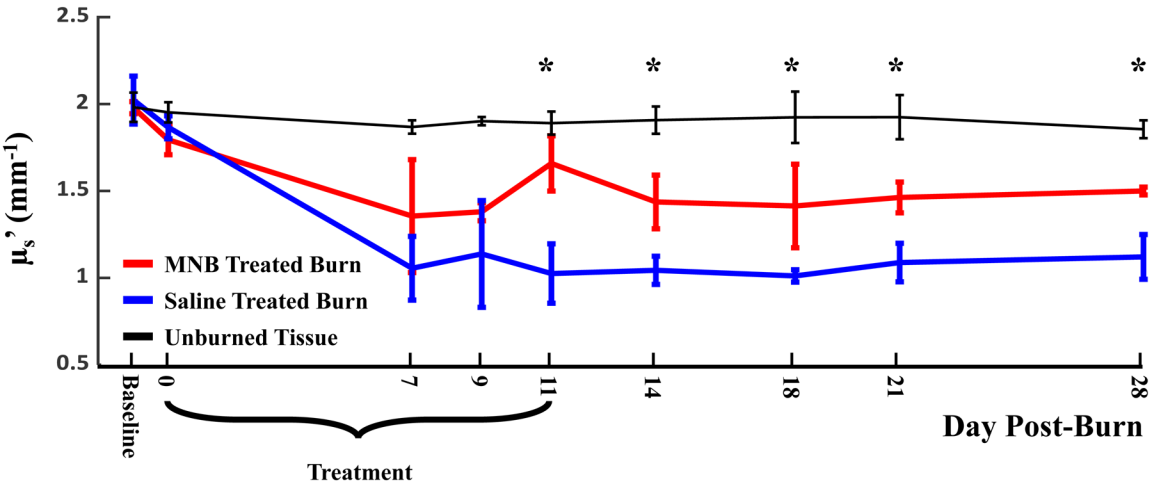

Figure 4:

Graphical representation of reduced scattering coefficient (ms') values for all animals treated with MNB(O_2) (red), Saline (blue), and unburned skin controls (black). Statistically significant differences *($p<0.05$)* between MNB(O_2) vs. Saline are denoted by *.

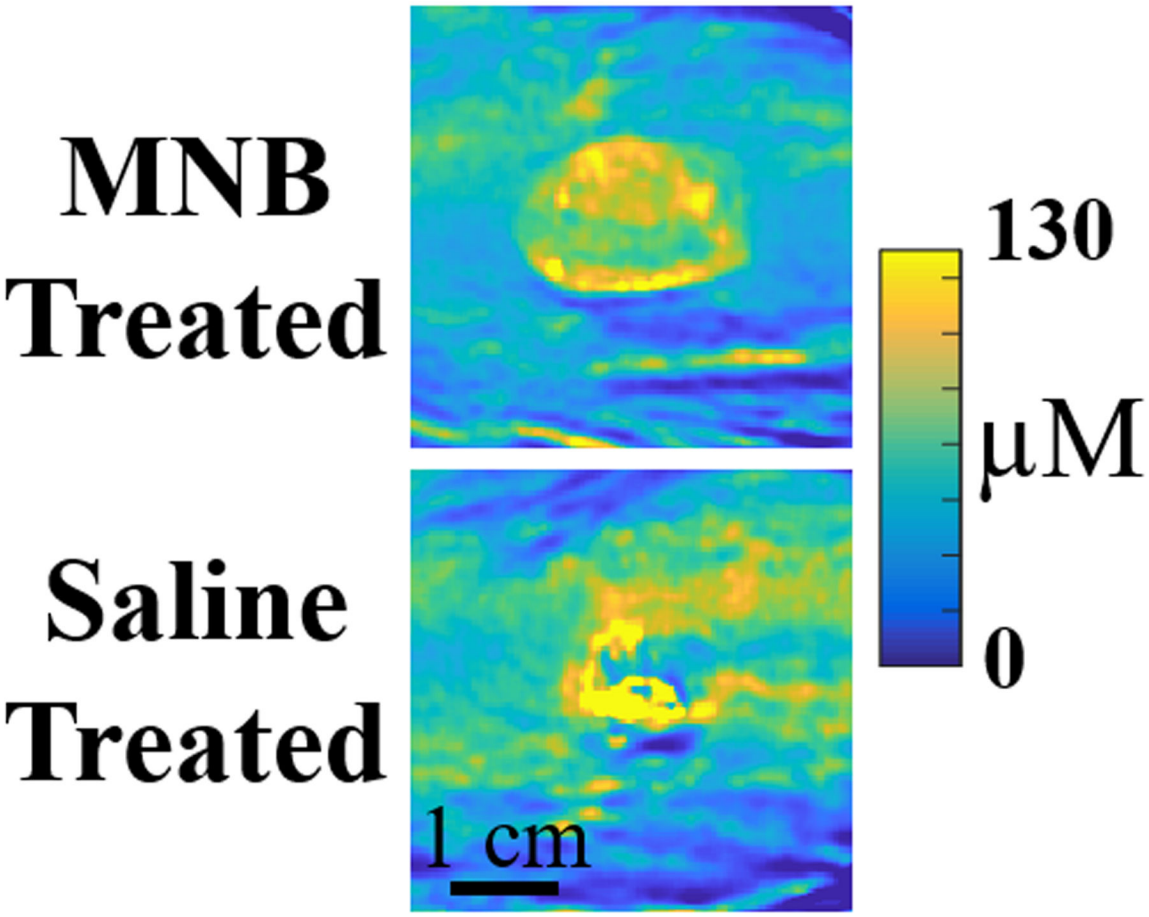

Figure 5:
Optical property maps of $cHbO_2$ concentration for MNB(O_2) and saline treated burns at day 14. For bar graphs of $cHbO_2$ measurements and optical property maps of $cHBO_2$ concentration for MNB(O_2) and saline treated burns at day 2,14, 21 and 28 please see Supplemental Digital Content 2.

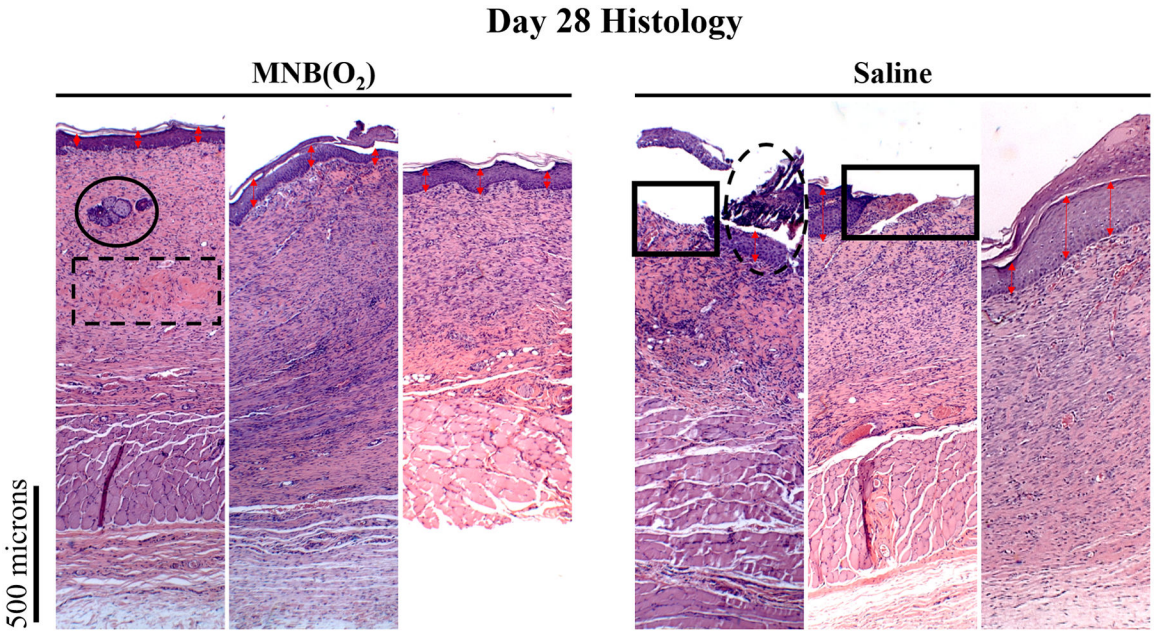

Figure 6:

H&E stains of sections from MNB(O_2) and saline-treated burns on day 28 at 25x magnification. Circled regions demarcate areas of hair follicle regeneration, dotted regions demarcate areas of collagen maturation and the solid rectangle demarcates areas of poor re-epithelization. Red arrows measure thickness of the epidermis.

Table 1:

P-values comparing mean reduced scattering values between MNB(O_2) and saline treated burn wounds. Statistically significant differences *($p<0.05$)* between MNB(O_2) vs. Saline are denoted by *

Treatment Day	Pre-Burn	0	7	9	11	14	18	21	28
Saline and Unburned	0.621	0.314	0.236	0.249	<0.01*	<0.05*	<0.05*	<0.05*	<0.01*